Tau inhibits mitochondrial calcium efflux and makes neurons vulnerable to calcium-induced cell death

Elena Britti[1], Joaquim Ros[1], Noemi Esteras[2]*, Andrey Y. Abramov[2]*

[1] Department of Ciencies Mediques Basiques. Institut de Recerca Biomedica, Universitat de Lleida, Spain

[2] Department of Clinical and Movement Neurosciences, UCL Institute of Neurology, Queen Square, London, United Kingdom

* Joint senior authors

Corresponding authors: Dr Noemi Esteras n.gallego@ucl.ac.uk ; or Prof Andrey Y. Abramov a.abramov@ucl.ac.uk

Highlights

- Tau induces cytosolic calcium oscillations in primary and iPSC-derived neurons
- Tau inhibits mitochondrial calcium efflux in neurons and astrocytes
- Tau inhibits mitochondrial NCLX
- Tau induces mitochondrial depolarization after calcium stimulation
- iPSC-neurons with a mutation in *MAPT* are more vulnerable to calcium-induced cell death

Abstract

Aggregation or phosphorylation of the microtubule-associated protein tau is the pathological hallmark in a number of diseases termed tauopathies, which include the most common neurodegenerative disorder, Alzheimer's disease; or frontotemporal dementia, linked to mutations in the gene *MAPT* encoding tau. Although misfolded tau has strong familial and histopathological (as in intracellular tangles) association with neurodegenerative disorders, the cellular mechanism of tau-induced pathology remains to be controversial. Here we studied the effect of tau on the cytosolic and mitochondrial calcium homeostasis using primary cortical cultures treated with the protein and iPSC-derived neurons bearing the 10+16 *MAPT* mutation linked to frontotemporal dementia. We found that incubation of the primary cortical co-cultures of neurons and astrocytes with tau induced spontaneous Ca^{2+} oscillations in the neurons, which were also observed in iPSC-neurons with the 10+16 *MAPT* mutation. Importantly, tau inhibited mitochondrial calcium efflux via the mitochondrial Na^{+}/Ca^{2+} exchanger (NCLX) in both neurons and astrocytes. This inhibition led to mitochondrial depolarisation in response to physiological and pathological calcium stimuli and made these cells vulnerable to calcium-induced caspase 3 activation and cell death. Thus, inhibition of the mitochondrial NCLX in neurons with misfolded or mutated tau can be involved in the mechanism of neurodegeneration.

Keywords:

Tau, mitochondrial calcium, NCLX, frontotemporal dementia, mitochondrial efflux

ABBREVIATIONS

$[Ca^{2+}]_c$ – Cytosolic calcium concentration

$[Ca^{2+}]_m$ – Mitochondrial calcium concentration

aCSF – Artificial cerebrospinal fluid

HBSS – Hank's Balanced Salt Solution

iPSC – induced pluripotent stem cells

mPTP – mitochondrial permeability transition pore

NCLX – Mitochondrial Na^+/Ca^{2+} exchanger

ROS – reactive oxygen species

1. INTRODUCTION

Tau protein plays an important physiological role in the assembly and stabilization of microtubules; and misfolding of this protein is involved in the pathogenesis of more than 20 different neurodegenerative disorders, termed tauopathies. Tauopathies include dementias such as Alzheimer's disease, where tau forms intracellular inclusions termed neurofibrillary tangles; or movement disorders such as progressive supranuclear palsy and corticobasal degeneration. The involvement of tau in the mechanism of neurodegeneration was confirmed by the identification of mutations in *MAPT* gene encoding tau, as the cause of frontotemporal dementia and parkinsonism linked to chromosome 17 (FTDP-17) [1].

Although tau is an intracellular protein, neurons can secrete and uptake tau, and monomers and aggregates of tau have been shown to be able to penetrate through biological membranes [2] and affect the function of cell organelles including mitochondria [3].

Mitochondria plays a major role as the energy producer in the cells; but it is also a main regulator of calcium signalling and a key element in the mechanism of cell death. Mitochondria is involved in the short Ca^{2+} buffering system protecting cytosol from overload; and in turn uses these calcium ions to activate mitochondrial respiration and ATP production. Mitochondria uptake Ca^{2+} through a specific calcium uniporter down the electrochemical gradient maintained across the mitochondrial membranes [4]. Efflux of Ca^{2+} out of the mitochondria is operated in exchange with H^+ in non-excitable cells or by a Na^+/Ca^{2+} exchanger [5] which was molecularly identified as NCLX [6]. Importantly, changes in the activity of the calcium uniporter or NCLX could lead to mitochondrial calcium overload, resulting in the opening of the mitochondrial permeability transition pore (mPTP) and triggering cell death [7]. We have previously shown that the deficiency [8] or mutation [9] in the Parkinson's-related *PINK1* gene led to inhibition of mitochondrial Ca^{2+} efflux, which resulted in vulnerability to calcium-dependent cell death. Importantly, inhibition of mitochondrial calcium efflux was also identified in cells with another familial form of Parkinson's disease – LRRK2 [10, 11]. Expression of wild type NCLX or phosphomimetic NCLX mutant to PINK1 or

LRRK2 deficient cells rescued the impaired mitochondrial Ca^{2+} extrusion and enhanced cell survival [12], confirming the importance of mitochondrial NCX in the mechanism of neurodegeneration in Parkinson's disease. Impaired mitochondrial calcium efflux has been also shown to play a role in the progression of Alzheimer's disease pathology [13]. Inhibited mitochondrial NCLX leads to the accumulation of Ca^{2+} in the matrix of mitochondria that can result in the triggering of the mitochondrial permeability transition pore in response to a physiological signal [14, 15]. Tau has been found to localize within the mitochondrial inner and outer membranes [16], is able to interact with mitochondrial transporters and complexes such as VDAC [17], or ATP synthase [18] and has in addition been shown to be involved in mitochondrial dysfunction resulting in mitochondrial ROS overproduction [19]. We suggest that tau can also modify cytosolic and mitochondrial calcium homeostasis. Here we found that incubation of cortical co –cultures of neurons and astrocytes with the tau K18 fragment for 24 hours induced spontaneous oscillations in $[Ca^{2+}]_c$ in the primary neurons. These oscillations lead to an increased basal level of mitochondrial calcium in tau-treated neurons compared to control cells. Induction of a cytosolic calcium signal in neurons with glutamate or astrocytes with ATP demonstrated the inhibition of the mitochondrial calcium efflux in the tau-treated cells, which showed a delayed Ca^{2+} efflux by the mitochondria in both cell types. This occurred due to the inhibition of the mitochondrial Na^+/Ca^{2+} exchanger (NCLX) by tau. As a consequence of the tau-induced inhibition of the mitochondrial calcium efflux, tau-treated cells and also iPSC-derived neurons with a mutation in *MAPT* presented an increased vulnerability to calcium-induced cell death, as shown by the increased mitochondrial depolarization and earlier caspase-3 activation in the presence of different triggers. These results offer a new perspective in understanding the mechanisms of tau-related neurodegeneration

2. MATERIALS AND METHODS

2.1. Cellular cultures

2.1.1. Primary cortical co-cultures of neurons and astrocytes were prepared from Sprague-Dawley rat pups (P2-P4) from the UCL breeding colony. Experimental procedures were performed in full compliance with the United Kingdom Animal (Scientific Procedures) Act of 1986 and with the European directive 2010/63/EU. Cortex was dissected and placed in ice-cold HBBS. Tissue was then trypsinized (Trypsin-EDTA 0.05%, ThermoFisher) for 15 min at 37°C, triturated and plated in coverslips that were previously coated with 0.05 mg/mL Poly-D-Lysine. Cultures were maintained in Neurobasal A medium, supplemented with B-27, GlutaMAX and in the presence of penicillin/streptomycin (all of them from ThermoFisher, Paisley, UK). Media was replaced after one week and cells were used at 12-16 DIV in all the experiments. Neurons were distinguished from glia by their morphology: while neurons present and smooth rounded soma and distinct processes, glial cells are bigger and flat and lay just below the focal plane of the neurons. In some experiments, neurons and glia were distinguished by their functionality due to their specific calcium-induced response to glutamate or ATP, respectively.

2.1.2. Human iPSC-derived neurons were generated and characterized as previously described [19, 20]. For the present experiments, three control cell lines were used: Control 1 was obtained from the laboratory of Dr Tilo Kunath, control 2 from the Coriell repository, and control 3 was purchased from Thermo Fisher Scientific. The two iPSC lines with the 10+16 *MAPT* mutation were generated by Dr. Selina Wray (UCL Institute of Neurology) from fibroblasts obtained from the National Hospital for Neurology and Neurosurgery, London, UK. All the experiments were performed in neurons ~ 120-150DIV.

2.2. Live-imaging

Unless otherwise specified, all the experiments were performed in HBSS buffer with Ca^{2+} and Mg^{2+} (ThermoFisher Scientific) supplemented with 10 mM HEPES, pH 7.4. In some cases, aCSF buffer was used (composition in mM: 125 NaCl, 2.5 KCl, 2 $MgCl_2$, 1.25 KH_2PO_4, 2 $CaCl_2$,

30 glucose and 25 HEPES, pH adjusted to 7.4). For the preparation of aCSF low magnesium, $MgCl_2$ was excluded from the media. Fluorescent dyes were obtained from ThermoFisher Scientific. Pseudo-intracellular media was used (composition in mM: 135 KCl, 10 NaCl, 20 HEPES, 5 pyruvate, 5 malate, 0.5 KH_2PO_4, 1 $MgCl_2$, 5 EGTA and 1.86 $CaCl_2$, to yield a free $[Ca^{2+}]$ of 100 nM; pH 7.1) during and after permeabilization of the cells with 20 µM digitonin.

For the simultaneous estimation of $[Ca^{2+}]_c$ and $[Ca^{2+}]_m$ cells were incubated with 5 µM Fluo-4-AM, 0.005% pluronic F-127 and 5 µM Rhod-5N for 30 min at rt and then washed. Images were obtained with a Zeiss 710 LSM confocal microscope with an integrated META detection system. Excitation of Fluo-4 and Rhod-5N was achieved with the 488 and 561 nm lasers respectively, and emitted light was measured at 500-550 nm and 580-620 nm (x40 objective). Mathematical analysis of calcium oscillations and decay rate were performed in Origin Pro 2018 (Origin Lab, USA)

The ratiometric calcium indicator Fura-2 AM was used in other experiments to monitor $[Ca^{2+}]_c$ alone or in combination with Rhod 123 to simultaneously measure mitochondrial membrane potential. Dyes were incubated for 30 min (Fura-2 AM 5 µM + 0.005% pluronic F-127) or 15 min (Rhod 123, 1 µM) at rt and washed. Fluorescence measurements were made on an epifluorescence inverted microscope equipped with a 20x fluorite objective (Nikon Eclipse Ti-S). Excitation light was provided by a xenon arc lamp, the beam passing a monochromator at 340 and 380 nm (Fura-2) and 490 nm (Rhod123) (Cairn Research, Kent, UK). Emitted fluorescence light was reflected through an ET510/80m filter to an Andor Zyla sCMOS camera (Cairn Research, Kent UK) and digitised to a 16-bit resolution. All imaging data were collected and analysed using Andor iQ2 (Andor, Belfast, UK) and Origin Pro 2018 (Origin Lab, USA) software.

Mitochondrial calcium efflux was analysed in permeabilized cells. Cells were loaded in HBSS media with 5 µM CoroNa green to visualize Na^+, 5 µM Rhod-5N to visualize Ca^{2+} and 0.005% pluronic F-127 for 30 min at rt and then washed. Cellular distribution of the fluorescence was

observed using a Zeiss 710 LSM confocal microscope with an integrated META detection system. Excitation of CoroNa Green and Rhod-5N was achieved with the 488 and 561 nm lasers respectively, and emitted light was measured at 500-550 nm and 580-620 nm (x40 objective). Cells were then permeabilized briefly with 20 μM digitonin in pseudo-intracellular buffer, which was afterwards washed and replaced with fresh pseudo-intracellular buffer for the duration of the experiment. To stimulate mitochondrial calcium uptake, $CaCl_2$ was applied to obtain a free [Ca^{2+}] concentration of 5 μM.

Assessment of apoptosis was done with NucView® 488 caspase-3 substrate (Biotium, California, USA) which allows the detection of caspase-3 activity in real time in individual cells. Cells were loaded for 15 min with 10 μM NucView. Live images were obtained with a Zeiss 710 LSM confocal microscope with an integrated META detection system. Samples were excited at 488 nm, and emitted light was collected at 500-550 nm. When the substrate (non-fluorescent) is cleaved by caspase-3, it forms a high-affinity DNA dye that stains the nucleus bright green, so a sudden increase in green fluorescence is detected in individual cells when caspase-3 is activated.

2.3 Statistics

Statistical analyses were performed in Origin Pro 2018. Two-tailed unpaired Student's t-test or one-way ANOVA followed by Bonferroni *post-hoc* test were used to estimate the statistical significance between experimental groups. A *p* value less than 0.05 was considered statistically significant for either test. Histograms are presented as mean±SEM**.**

3. RESULTS

3.1. Tau induces changes in cytosolic and mitochondrial Ca^{2+}

Primary cortical co-cultures of neurons and astrocytes were incubated for 24 hours with 300 nM tau K18 (from now on referred in the text as tau), which comprises the four repeat (4R) region of the protein [21]. This led to spontaneous calcium oscillations (shown by Fluo-4 indicator) and a slow elevation of the $[Ca^{2+}]_c$ of neurons (Fig. 1A-C).

Importantly, $[Ca^{2+}]_c$ oscillations were followed by mitochondrial calcium uptake (shown by Rhod-5N staining) and efflux at the time of the cytosolic calcium peaks, with a slow recovery of $[Ca^{2+}]_m$ (Fig. 1A, D). The analysis of the cytosolic calcium oscillations (Fig. 1B-C) revealed an increased number of occurrences (peaks) in tau-treated cells (Fig. 1E). The characteristics of these peaks included a significantly higher average area and height and lower FWHW (full width at half maximum) (Fig. 1F-H) in tau-treated cells.

The ability of tau to induce $[Ca^{2+}]_c$ changes in cortical neurons could also be observed in human cortical neurons derived from iPSC with the 10+16 mutation in *MAPT* gene, which leads to an overproduction of 4R tau, and is linked to frontotemporal dementia [20]. At D150, the patient's neurons showed spontaneous $[Ca^{2+}]_c$ oscillations while control neurons did not induce any spontaneous calcium changes of this altitude or frequency (Figure 1 I-J).

Thus, accumulation of tau induces changes in $[Ca^{2+}]_c$ of neurons that also modulate mitochondrial calcium signal. Interestingly, acute stimulation of the primary cultures with K18 tau didn't induce any calcium signals in the neurons (data not shown). This might suggest either that these effects are not the result of an immediate or direct effect of this tau fragment on the cells; or that a cellular modification of the protein (e.g. uptake, aggregation, phosphorylation) is necessary. Further investigation will be essential to understand the exact mechanisms/structures by which tau alters the calcium homeostasis.

3.2 Tau modifies glutamate-induced calcium signal in neurons

Glutamate is the major excitatory neurotransmitter and the calcium-induced response to low concentrations of glutamate (0.5-5μM) is a functional characteristic of neurons. Application of 5 μM glutamate to control primary neurons induced a typical peak-like elevation of $[Ca^{2+}]_c$ (Figure 2A). However, application of the same concentration of glutamate to primary cortical neurons pre-incubated for 24 hours with tau (300 nM) produced an increase in $[Ca^{2+}]_c$ which was different to control (Figure 2A). Although tau pre-incubation did not significantly changed the rate of calcium influx or the amplitude of the glutamate-induced calcium signal measured

with Fluo-4 (Fig. 2B, C); it significantly altered the cytosolic calcium efflux (Fig. 2 A, E). Neurons pre-treated with tau presented a significantly higher calcium efflux half time (Fig. 2E), indicating that these neurons needed ~1.5x times to drop the $[Ca^{2+}]_c$ to 50% of the peak, when compared to the controls.

3.3 Tau inhibits mitochondrial calcium efflux in neurons

Glutamate-induced cytosolic calcium elevation (Fig. 2A) induces Ca^{2+} uptake by the mitochondria (Fig. 2F). Pre-incubation of the cells with K18 tau for 24 hours significantly modified the glutamate-induced changes in $[Ca^{2+}]_m$. Although tau induced a significant increase in the amplitude of mitochondrial calcium uptake (Fig. 2H), it also effectively inhibited mitochondrial calcium efflux (Figure 2 F, I-J). Notably, both parameters indicating an inhibition of the rate of calcium efflux (Rhod-5N K decay rate, Fig. 2I; and Rhod-5N half life, Fig. 2J) were significantly lower and higher, respectively, in neurons treated with tau.

Thus, incubation of primary cortical neurons with tau inhibited mitochondrial calcium efflux independently of the amplitude of uptake of Ca^{2+}.

3.4 Tau inhibits mitochondrial calcium efflux in astrocytes

Calcium signalling in astrocytes can be on the other hand mediated by different messengers such as ATP, which is able to activate P2Y receptors on the membrane of the glial cells and induce an increase in the $[Ca^{2+}]_c$. Stimulation of primary co-cultures of neurons and astrocytes with 100 μM ATP specifically induced a typical cytosolic calcium signal in the astrocytes (Fig. 3A), which was different in the cultures pre-treated with tau K18 300 nM for 24 hours (Fig. 3A-E).

Importantly, the cytosolic calcium peak was accompanied by calcium uptake in the mitochondria, as measured simultaneously with Rhod-5N (Fig 3F). Mitochondrial calcium homeostasis was also different in the astrocytes (Fig. 3F-J), in which tau-pretreatment inhibited the mitochondrial calcium efflux, in a similar way to what we observed in the neurons (Fig. 2F-J). Both $_mCa^{2+}$ efflux K decay rate (Fig. 3I) and half life (Fig. 3J) were significantly

altered in the tau-treated astrocytes, confirming the slower recovery of the basal $[Ca^{2+}]_m$ compared to the control.

This result suggests that inhibition of the mitochondrial efflux by tau is not restricted to the neurons, but appears to be a more general phenomenon occurring in both cellular types in primary cortical co-cultures.

3.5 Tau inhibits mitochondrial NCLX

To further investigate the tau-induced altered mitochondrial calcium efflux, we studied the mitochondrial Ca^{2+} handling after permeabilizing the primary cultures and exposing the mitochondria to $CaCl_2$ (final free $[Ca^{2+}]$ was 5 μM). As observed in Figure 4B, while in controls $CaCl_2$ induced a $_m[Ca^{2+}]$ peak followed by a quickly recover of basal $[Ca^{2+}]_m$ in cells treated with tau K18 the calcium efflux was impaired and resembled the one observed when treating the control cells with the mitochondrial sodium/calcium exchanger (NCLX) inhibitor CPG-37157 (10 μM) (Fig. 4B). Indeed, mitochondrial NCLX is the main responsible for mitochondrial calcium extrusion in the neurons. This exchanger works by extruding Ca^{2+} from the mitochondrial matrix using the electrochemical gradient for Na^+ entry in the mitochondria. To investigate its function, we loaded the primary cultures with the sodium indicator CoroNa Green together with the mitochondrial calcium indicator Rhod-5N and permeablized the cells using digitonin as described in Methods (Fig. 4A). Subsequent application of $CaCl_2$ to the mitochondria led to an increase in $[Ca^{2+}]_m$ followed by a gradual decrease which was paralleled by a decrease and subsequent increase in $[Na^+]_m$ as NCLX exchanged both ions in control cells (Fig. 4C). In contrast, in cells treated with tau (Fig. 4D), the peak induced by $CaCl_2$ was followed by an altered $[Ca^{2+}]_m$ efflux and $[Na^+]_m$ influx, indicating that tau induces the impairment of the exchanger thus inhibiting the mitochondrial calcium efflux.

3.6 Calcium-induced mitochondrial depolarisation in iPSC-neurons with tau pathology

Tau-induced inhibition of mitochondrial calcium efflux might lead to pathological consequences for the neurons through different mechanisms. We first tested if the tau-induced calcium impairment could alter mitochondrial membrane potential using iPSC-derived neurons from patients with the 10+16 mutation in *MAPT* gene. Application of a physiological concentration of glutamate (5 µM) to the human iPSC-derived cortical neurons induced a typical increase in $[Ca^{2+}]_c$ in control cells (Fig. 5A). Simultaneous measurement of mitochondrial membrane potential (Rhodamine123 was taken as indicator) show no significant changes in control cells (Figure 5A, D). However, application of the same trigger to iPSC-derived neurons of patients with the *MAPT* mutation led to changes in the shape of the cytosolic calcium signal - in agreement with the responses observed in the primary neurons treated with K18 tau (Fig. 2A); and, importantly, significant mitochondrial depolarisation (Fig. 5 B-D). As shown in the representative traces in Fig. 5 B, C; the sustained $[Ca^{2+}]_c$ increases in the neurons with tau pathology correlated with the mitochondrial depolarization. This suggests that the inhibition of mitochondrial calcium efflux could result in the depolarization of the mitochondria in cells with tau pathology, even in the presence of a physiological stimulus such as the application of a low dose of glutamate.

Application of 1 µM FCCP at the end of the experiment serves as a positive control to induce a complete mitochondrial depolarization, and at the same time induces the release of Ca^{2+} from the mitochondria to the cytosol. Elevation of $[Ca^{2+}]_c$ in response to FCCP could be therefore used as an indirect measurement of the mitochondrial calcium pool. Quantification of the amplitude of this response showed however, no differences between control and *MAPT* mutation groups (Fig. 5E), indicating that there were no significant changes in the mitochondrial calcium content between both groups after a physiological calcium stimulus.

3.7 Repetitive calcium elevation leads to mitochondrial depolarisation in neurons pre-treated with tau

In the suggested scenario of inhibited mitochondrial calcium efflux, the requirement for frequent mitochondrial calcium uptake might induce mitochondrial calcium overload and lead

as well to mitochondrial depolarisation. One well-known cellular model to prove this hypothesis is the low magnesium model of epilepsy in which the removal of Mg^{2+} from the cellular media leads to repetitive cytosolic calcium peaks induced by glutamate release, that challenge the capacity of the mitochondria as a Ca^{2+}- buffering organelle [22, 23]. As shown in Fig. 6A, the removal of Mg^{2+} from the media induced repetitive $_{c}Ca^{2+}$ oscillations in the neurons, and a progressive increase in the basal calcium levels, which was much more dramatic when the cells had been pre-incubated with tau K18 (Fig. 6B). More importantly, not only the incubation of primary cortical neurons with tau changed the shape of the calcium signal induced by omitting of Mg^{2+}, but also increased significantly the mitochondrial depolarisation rate in response to this stimulus (Figure 6 A-C). Thus, incubation of the neurons with tau and inhibition of the mitochondrial calcium efflux results in mitochondrial depolarisation in response to repetitive calcium stimulation.

3.8 Mitochondrial calcium overload leads to earlier caspase 3 activation in cells with the 10+16 *MAPT* mutation

Mitochondrial calcium overload is an important trigger for the opening of the mitochondrial permeability transition pore (mPTP), and the induction of cell death in many diseases. For this reason, we next explored the susceptibility of control and tau-mutated iPSC-derived neurons to the opening of the mPTP and the induction of cell death under different triggers. We first tested if a glutamate-induced calcium influx was enough to provoke the opening of the mPTP and induce apoptosis. To test this, we monitored caspase-3 activation with the indicator NucView in live cells exposed to a high dose of glutamate (50 μM). As shown in Fig. 7, glutamate stimulation was not sufficient to trigger mPTP opening and caspase-3 activation in either control or patient iPSC-neurons. It is known that the electrogenic calcium inonophore ferutinin [24] induces mitochondrial calcium overload and the opening of mPTP followed by induction of cell death [25]. Exposition of the iPSC-neurons to 50μM ferutinin indeed induced the activation of caspase 3 and apoptosis in both control and tau-mutated human iPSC derived neurons (Fig. 7). However, importantly, in control cells the time from application of ferutinin to

caspase 3 activation was significantly longer compared to patient's cells (Fig. 7A-B), indicating an increased susceptibility of the patient cells to the mPTP opening and apoptosis activation induced by calcium overload. Thus, this result suggests that inhibition of mitochondrial calcium efflux by tau makes these cells more vulnerable to calcium-induced cell death.

4. DISCUSSION

Here we show that tau is able to alter the cellular calcium homeostasis both in primary cells treated extracellularly with the protein and in neurons with an intrinsic tau pathology, such as human iPSC-derived neurons bearing a mutation in the gene *MAPT* encoding tau. In both cases, tau induced changes in cytosolic Ca^{2+} mostly in the form of calcium oscillations. This effect could be produced by a number of factors including alterations in the activity of glutamate receptors, changes in the plasma membrane potential and triggering of voltage-gated calcium channels etc.

Stimulation of neurons (with glutamate) and astrocytes (with ATP) induced a typical cytosolic calcium peak followed by mitochondrial calcium uptake. In our experiments, we show that tau induced the inhibition of the subsequent mitochondrial calcium efflux. Additionally, experiments in permeabilized cells showed the impairment of both the $[Ca^{2+}]_m$ efflux and the parallel $[Na^+]_m$ influx in cells treated with tau. Although for mitochondria in neurons several possible mitochondrial exchangers have been suggested to extrude Ca^{2+} (expression of NCX1-3; NCLX), all of them produce exchange of Na^+ to Ca^{2+} [14, 26, 27], so we propose that tau pathology induces the inhibition of mitochondrial NCLX.

Tau-induced inhibition of the calcium efflux in mitochondria results in a slower mitochondrial efflux that makes cells vulnerable to fast repetitive calcium fluxes. Our experiments with both an epileptic-like stimulus and with the electrogenic calcium ionophore ferutinin confirm that cells with tau pathology have an increased vulnerability to calcium-induced pathology; inducing mitochondrial depolarization and apoptotic processes faster than control cells.

Modification of the activity of mitochondrial NCLX might affect general mitochondrial function. Physiological mitochondrial calcium uptake stimulates dehydrogenases in the electron transport chain [28] and can induce a mild hyperpolarisation of the inner mitochondrial membrane. However, in our experiments, neurons with the 10+16 *MAPT* mutation underwent mitochondrial depolarisation in response to a small concentration of glutamate (Figure 4) that suggest an inhibitory effect of the delayed calcium efflux on mitochondrial respiration.

The activity of the exchanger is dependent on a number of factors including ΔΨm [12]. The inhibitory effect of tau on this transporter is less likely dependent on the effect of the protein on mitochondrial membrane potential since as we have previously shown, tau is associated with an increase in ΔΨm in the 10+16 *MAPT* iPSC-derived neurons [19].

Another possible explanation of tau effect on mitochondrial calcium efflux could be the induction of the sporadic cytosolic calcium oscillations caused by tau in neurons. Constant calcium influx could potentially overload mitochondria, resulting in the inhibition of the efflux upon the stimulation of cells with a more profound calcium signal. However, the indirect measurement of the mitochondrial Ca^{2+} pool as changes in $[Ca^{2+}]_c$ induced by the calcium release from the mitochondria after application of FCCP (Fig. 4) showed no difference between control and cells with 10+16 *MAPT* mutation, potentially excluding this mechanism of NCLX inhibition at least with the physiological stimulus tested in that experiment. Additional experiments will be required to better understand the specific mechanism by which tau inhibits mitochondrial NCLX.

Development of the strategy of protection of the cells against calcium induced cell death is one of the fast-developing field of research. The major ways for protection are: a) inhibiting of mPTP, b) partial inhibition of mitochondrial calcium uptake [29] or c) activation of NCLX [10, 12, 30]. Although using of any of this strategy could bring to potential protection of the cells, most promising protection could be expected in more targeted to damaged pathways, like in case of tau – activation of NCLX.

5. CONCLUSIONS

To our knowledge, up to date very few studies have focused on analysing the role of tau in regulating mitochondrial calcium. Here we provide evidence that both exogenous and endogenous tau are able to alter neuronal calcium homeostasis. Tau-induced inhibition of mitochondrial calcium efflux increases the vulnerability of neurons to calcium-induced cell death, indicating that targeting of mitochondrial NCLX could be a potential new strategy for tauopathies.

6. ACKNOWLEDGEMENTS

We would like to thank Dr. Seema Qamar from Cambridge University for providing with K18 tau fragment; and Dr. Selina Wray from University College London who generated the iPSC lines of the patients with the 10+16 *MAPT* mutation.

7. FUNDING

EB was supported with an EMBO short-term fellowship (number 7834) for the development of this project. The work was supported by EPSRC grant EP/R024898/1.

Author Contribution Section

EB, NE perform the experiments; EB, NE, JR, AYA analysed data; AYA and NE wrote the manuscript; JR, NE, EB and AYA corrected the manuscript.

FIGURE LEGENDS

Fig. 1 Tau induces calcium oscillations in neuronal cells

A. Representative images of cytosolic (Fluo-4, green) and mitochondrial (Rhod-5N, red) [Ca^{2+}] of cells treated with tau. Scale bar 20 µm. Arrows indicate an example of the cytosolic and mitochondrial regions selected for the quantification. **B, C**. Cytosolic calcium oscillations occurring in individual neurons incubated with K18 tau (C) for 24 hours as compared with control neurons (B). Graph shows n=9 control cells, n=8 tau representative cells presenting calcium oscillations. **D.** Representative traces showing calcium oscillations in the cytosol (as stained by Fluo-4, green) and mitochondria (as stained by Rhod-5N, red) of neurons treated with K18 tau for 24 hours. **E-H.** Histograms represent the average±SEM of the characteristics of the different peaks occurring in B, C: (**E**, number of occurences (peaks) happening in 110s; **F**, peak area; **G**, peak height, **H**, peak FWHW) n= 96 control, 315 tau. ***p<0.001, unpaired Student's t-test. **I, J.** Calcium oscillations (measured with Fura-2) occurring in iPSC-derived neurons (D150) with the 10+16 mutation in MAPT encoding tau protein **(J)**, as compared to a healthy control at the same age **(I)**.

Fig. 2. Tau modifies glutamate-induced calcium signals and inhibits mitochondrial calcium efflux in neurons

A. Representative experiment showing the changes in cytosolic calcium measured with Fluo-4 in response to glutamate 5 µM in control primary cortical neurons and cells treated with 300 nM K18 tau for 24 hours. Traces show the average±SEM of control n=10, tau n=9 cells. **B-E** Histograms show average±SEM of different features of the glutamate-induced calcium response in control (n=34) and tau-treated cells (n=69): rate of calcium influx in the cytosol (**B**); amplitude of the peak **(C)**; and decay rate **(D)** and half life **(E)** of the calcium efflux. * p<0.05, unpaired Student's t-test. **F.** Traces show the changes in mitochondrial calcium measured with Rhod-5N after a cytosolic calcium influx induced by glutamate 5 µM in control primary cortical neurons and cells treated with 300 nM K18 tau for 24 hours (average±SEM of control n=30, tau n=53). **G-J** Histograms show average±SEM of different features of the

mitochondrial calcium changes in control (n=30) and tau-treated cells (53): rate of calcium influx in the mitochondria **(G)**; amplitude of the peak **(H)**; and decay rate **(I)** and half life **(J)** of the calcium efflux. * p<0.05, unpaired Student's t-test.

Fig. 3. Tau modifies ATP-induced calcium signals and inhibits mitochondrial calcium efflux in astrocytes

A. Graph shows the changes in $[Ca^{2+}]_c$ in response to 100 µM ATP in astrocytes treated or not with tau K18 300 nM for 24 hours. Traces represent the average±SEM of control n=149, tau=178. **B-E.** Histograms depict the average±SEM of different features of the traces averaged in A: rate of calcium influx in the cytosol **(B)**; amplitude of the peak **(C)**; and decay rate **(D)** and half life **(E)** of the calcium efflux. *** p<0.001, unpaired Student's t-test. **F.** Graph shows the changes in $[Ca^{2+}]_m$ after the cytosolic calcium influx induced by 100 µM ATP in control primary cortical astrocytes treated or not with tau K18 300 nM for 24 hours. Traces represent the average±SEM of control n=165, tau=70. **G-J.** Histograms depict the average±SEM of different features of the traces averaged in G: rate of calcium influx in the mitochondria **(G)**; amplitude of the peak **(H)**; and decay rate **(I)** and half life **(J)** of the calcium efflux. ** p<0.01; *** p<0.001, unpaired Student's t-test.

Fig. 4. Tau inhibits mitochondrial NCLX

A. Representative images showing the sodium (CoroNa Green, green) and mitochondrial calcium staining (red, Rhod-5N) in primary cultures before and after cellular permeabilization with 60 µM digitonin. Note the mitochondrial location of the dyes after the permeabilization of the plasma membrane. Scale bar: 20 µm. **B.** Representative traces showing $[Ca^{2+}]_m$ changes (as indicated by Rhod-5N fluorescence) in permeabilized cells of control, control treated with the mitochondrial NCLX inhibitor CGP-37157 and tau-treated cells. **C-D.** Representative traces showing parallel $[Ca^{2+}]_m$ (Rhod-5N fluorescence) and $[Na^{+}]_m$ (CoroNa Green fluorescence) changes in permeabilized control (C) and tau-treated (D) cells to study

mitochondrial NCLX function. Experiments were repeated at least 3 times in all the cases in different coverslips.

Fig. 5. Calcium-induced mitochondrial depolarization in iPSC-neurons with tau pathology

A-C. Traces show the simultaneous measurement of $[Ca^{2+}]_c$ with Fura-2 and mitochondrial membrane potential with Rhod 123 in representative individual iPSC-derived neurons of a healthy control **(A)** and 2 patients with the *MAPT* 10+16 mutation **(B,C)**. Glutamate 5 µM was used to induce a calcium influx in the cytosol and FCCP 1 µM as an uncoupler to fully depolarize the mitochondria. Sustained increases in $[Ca^{2+}]_c$ correlate with mitochondrial depolarization. **D.** Histogram shows the average±SEM of the % of mitochondrial depolarization after the glutamate-induced calcium influx (control 1, n=518; control 2, n=305; control 3, n=554; patient 1, n=605; patient 2, n=1144). Data was normalized so basal levels represented 0% mitochondrial depolarization and response to FCCP represents 100%. ***p<0.001, one-way ANOVA with Bonferroni means comparisons. **E.** Histogram shows the average±SEM of the amplitude of the $[Ca^{2+}]_c$ increase after mitochondrial depolarization with FCCP, as an indirect measurement of the $[Ca^{2+}]_m$ released from the mitochondria (control 1, n=887; control 2, n=470; control 3, n=810; patient 1, n=735; patient 2, n=1495).

Fig. 6. Repetitive calcium elevation leads to mitochondrial depolarisation in neurons pre-treated with tau

A-B. Traces show the simultaneous measurement of $[Ca^{2+}]_c$ with Fura-2 and mitochondrial membrane potential with Rhod 123 in representative individual primary cortical control neurons **(A)** and neurons pre-incubated with K18 tau 300 nM for 24 hours **(B)**. Replacement of aCSF media with low magnesium aCSF media at the indicated time-point induced cytosolic repetitive signals in the neurons due to glutamate release. FCCP was applied at the end to fully depolarize the mitochondria. **C.** Histogram represents the average±SEM of the rate of

mitochondrial depolarization (increase in Rhod 123 signal) after Mg^{2+} removal in control and tau neurons. (control, n=60 tau, n=91). ***p<0.001, unpaired Student's t-test.

Fig. 7. Mitochondrial calcium overload leads to earlier caspase 3 activation in cells with 10+16 *MAPT* mutation

A. Representative traces of iPSC-derived neurons from a healthy control and 2 carriers of the *MAPT* 10+16 mutation showing caspase-3 activation in response to ferutinin as indicated by the sudden increase in NucView fluorescence intensity. **B.** Histogram represents the average±SEM of the time from ferutinin application to caspase-3 activation in n= 206 control, 304 patient 1 and 422 patient 2 neurons. ***p<0.001, one-way ANOVA with Bonferroni means comparisons.

8. REFERENCES

[1] C. Dumanchin, A. Camuzat, D. Campion, P. Verpillat, D. Hannequin, B. Dubois, P. Saugier-Veber, C. Martin, C. Penet, F. Charbonnier, Y. Agid, T. Frebourg, A. Brice, Segregation of a missense mutation in the microtubule-associated protein tau gene with familial frontotemporal dementia and parkinsonism, Hum Mol Genet, 7 (1998) 1825-1829.

[2] L.D. Evans, T. Wassmer, G. Fraser, J. Smith, M. Perkinton, A. Billinton, F.J. Livesey, Extracellular Monomeric and Aggregated Tau Efficiently Enter Human Neurons through Overlapping but Distinct Pathways, Cell Rep, 22 (2018) 3612-3624.

[3] C.A. Lasagna-Reeves, D.L. Castillo-Carranza, U. Sengupta, A.L. Clos, G.R. Jackson, R. Kayed, Tau oligomers impair memory and induce synaptic and mitochondrial dysfunction in wild-type mice, Mol Neurodegener, 6 (2011) 39.

[4] Y. Kirichok, G. Krapivinsky, D.E. Clapham, The mitochondrial calcium uniporter is a highly selective ion channel, Nature, 427 (2004) 360-364.

[5] E. Carafoli, R. Tiozzo, G. Lugli, F. Crovetti, C. Kratzing, The release of calcium from heart mitochondria by sodium, J Mol Cell Cardiol, 6 (1974) 361-371.

[6] R. Palty, W.F. Silverman, M. Hershfinkel, T. Caporale, S.L. Sensi, J. Parnis, C. Nolte, D. Fishman, V. Shoshan-Barmatz, S. Herrmann, D. Khananshvili, I. Sekler, NCLX is an essential component of mitochondrial Na+/Ca2+ exchange, Proc Natl Acad Sci U S A, 107 (2010) 436-441.

[7] R. Abeti, A.Y. Abramov, Mitochondrial Ca(2+) in neurodegenerative disorders, Pharmacol Res, 99 (2015) 377-381.

[8] S. Gandhi, A. Wood-Kaczmar, Z. Yao, H. Plun-Favreau, E. Deas, K. Klupsch, J. Downward, D.S. Latchman, S.J. Tabrizi, N.W. Wood, M.R. Duchen, A.Y. Abramov, PINK1-associated Parkinson's disease is caused by neuronal vulnerability to calcium-induced cell death, Mol Cell, 33 (2009) 627-638.

[9] A.Y. Abramov, M. Gegg, A. Grunewald, N.W. Wood, C. Klein, A.H. Schapira, Bioenergetic consequences of PINK1 mutations in Parkinson disease, PLoS One, 6 (2011) e25622.

[10] M.H.R. Ludtmann, M. Kostic, A. Horne, S. Gandhi, I. Sekler, A.Y. Abramov, LRRK2 deficiency induced mitochondrial Ca(2+) efflux inhibition can be rescued by Na(+)/Ca(2+)/Li(+) exchanger upregulation, Cell Death Dis, 10 (2019) 265.

[11] M. Verma, J. Callio, P.A. Otero, I. Sekler, Z.P. Wills, C.T. Chu, Mitochondrial Calcium Dysregulation Contributes to Dendrite Degeneration Mediated by PD/LBD-Associated LRRK2 Mutants, J Neurosci, 37 (2017) 11151-11165.

[12] M. Kostic, M.H. Ludtmann, H. Bading, M. Hershfinkel, E. Steer, C.T. Chu, A.Y. Abramov, I. Sekler, PKA Phosphorylation of NCLX Reverses Mitochondrial Calcium Overload and

Depolarization, Promoting Survival of PINK1-Deficient Dopaminergic Neurons, Cell Rep, 13 (2015) 376-386.

[13] P. Jadiya, D.W. Kolmetzky, D. Tomar, A. Di Meco, A.A. Lombardi, J.P. Lambert, T.S. Luongo, M.H. Ludtmann, D. Pratico, J.W. Elrod, Impaired mitochondrial calcium efflux contributes to disease progression in models of Alzheimer's disease, Nat Commun, 10 (2019) 3885.

[14] A. Wood-Kaczmar, E. Deas, N.W. Wood, A.Y. Abramov, The role of the mitochondrial NCX in the mechanism of neurodegeneration in Parkinson's disease, Adv Exp Med Biol, 961 (2013) 241-249.

[15] S. Gandhi, A. Vaarmann, Z. Yao, M.R. Duchen, N.W. Wood, A.Y. Abramov, Dopamine induced neurodegeneration in a PINK1 model of Parkinson's disease, PLoS One, 7 (2012) e37564.

[16] D. Cieri, M. Vicario, F. Vallese, B. D'Orsi, P. Berto, A. Grinzato, C. Catoni, D. De Stefani, R. Rizzuto, M. Brini, T. Cali, Tau localises within mitochondrial sub-compartments and its caspase cleavage affects ER-mitochondria interactions and cellular Ca(2+) handling, Biochim Biophys Acta Mol Basis Dis, 1864 (2018) 3247-3256.

[17] M. Manczak, P.H. Reddy, Abnormal interaction of VDAC1 with amyloid beta and phosphorylated tau causes mitochondrial dysfunction in Alzheimer's disease, Hum Mol Genet, 21 (2012) 5131-5146.

[18] C. Liu, X. Song, R. Nisbet, J. Gotz, Co-immunoprecipitation with Tau Isoform-specific Antibodies Reveals Distinct Protein Interactions and Highlights a Putative Role for 2N Tau in Disease, J Biol Chem, 291 (2016) 8173-8188.

[19] N. Esteras, J.D. Rohrer, J. Hardy, S. Wray, A.Y. Abramov, Mitochondrial hyperpolarization in iPSC-derived neurons from patients of FTDP-17 with 10+16 MAPT mutation leads to oxidative stress and neurodegeneration, Redox Biol, 12 (2017) 410-422.

[20] T. Sposito, E. Preza, C.J. Mahoney, N. Seto-Salvia, N.S. Ryan, H.R. Morris, C. Arber, M.J. Devine, H. Houlden, T.T. Warner, T.J. Bushell, M. Zagnoni, T. Kunath, F.J. Livesey, N.C. Fox, M.N. Rossor, J. Hardy, S. Wray, Developmental regulation of tau splicing is disrupted in stem cell-derived neurons from frontotemporal dementia patients with the 10 + 16 splice-site mutation in MAPT, Hum Mol Genet, 24 (2015) 5260-5269.

[21] M. Kjaergaard, A.J. Dear, F. Kundel, S. Qamar, G. Meisl, T.P.J. Knowles, D. Klenerman, Oligomer Diversity during the Aggregation of the Repeat Region of Tau, ACS Chem Neurosci, 9 (2018) 3060-3071.

[22] S. Kovac, A.M. Domijan, M.C. Walker, A.Y. Abramov, Prolonged seizure activity impairs mitochondrial bioenergetics and induces cell death, J Cell Sci, 125 (2012) 1796-1806.

[23] S. Kovac, E. Preza, H. Houlden, M.C. Walker, A.Y. Abramov, Impaired Bioenergetics in Mutant Mitochondrial DNA Determines Cell Fate during Seizure-Like Activity, Mol Neurobiol, 56 (2019) 321-334.

[24] M.V. Zamaraeva, A.I. Hagelgans, A.Y. Abramov, V.I. Ternovsky, P.G. Merzlyak, B.A. Tashmukhamedov, A.I. Saidkhodzjaev, Ionophoretic properties of ferutinin, Cell Calcium, 22 (1997) 235-241.

[25] A.Y. Abramov, M.R. Duchen, Actions of ionomycin, 4-BrA23187 and a novel electrogenic Ca2+ ionophore on mitochondria in intact cells, Cell Calcium, 33 (2003) 101-112.

[26] A. Scorziello, C. Savoia, A. Secondo, F. Boscia, M.J. Sisalli, A. Esposito, A. Carlucci, P. Molinaro, L. Lignitto, G. Di Renzo, A. Feliciello, L. Annunziato, New insights in mitochondrial calcium handling by sodium/calcium exchanger, Adv Exp Med Biol, 961 (2013) 203-209.

[27] A. Verkhratsky, M. Trebak, F. Perocchi, D. Khananshvili, I. Sekler, Crosslink between calcium and sodium signalling, Exp Physiol, 103 (2018) 157-169.

[28] R.M. Denton, J.G. McCormack, The calcium sensitive dehydrogenases of vertebrate mitochondria, Cell Calcium, 7 (1986) 377-386.

[29] P.R. Angelova, D. Vinogradova, M.E. Neganova, T.P. Serkova, V.V. Sokolov, S.O. Bachurin, E.F. Shevtsova, A.Y. Abramov, Pharmacological Sequestration of Mitochondrial Calcium Uptake Protects Neurons Against Glutamate Excitotoxicity. Mol Neurobiol, 56 (2019) 2244-2255.

[30] M.H.R. Ludtmann, A.Y. Abramov, Mitochondrial calcium imbalance in Parkinson's disease. Neurosci Lett 10 (2018) 86-90.

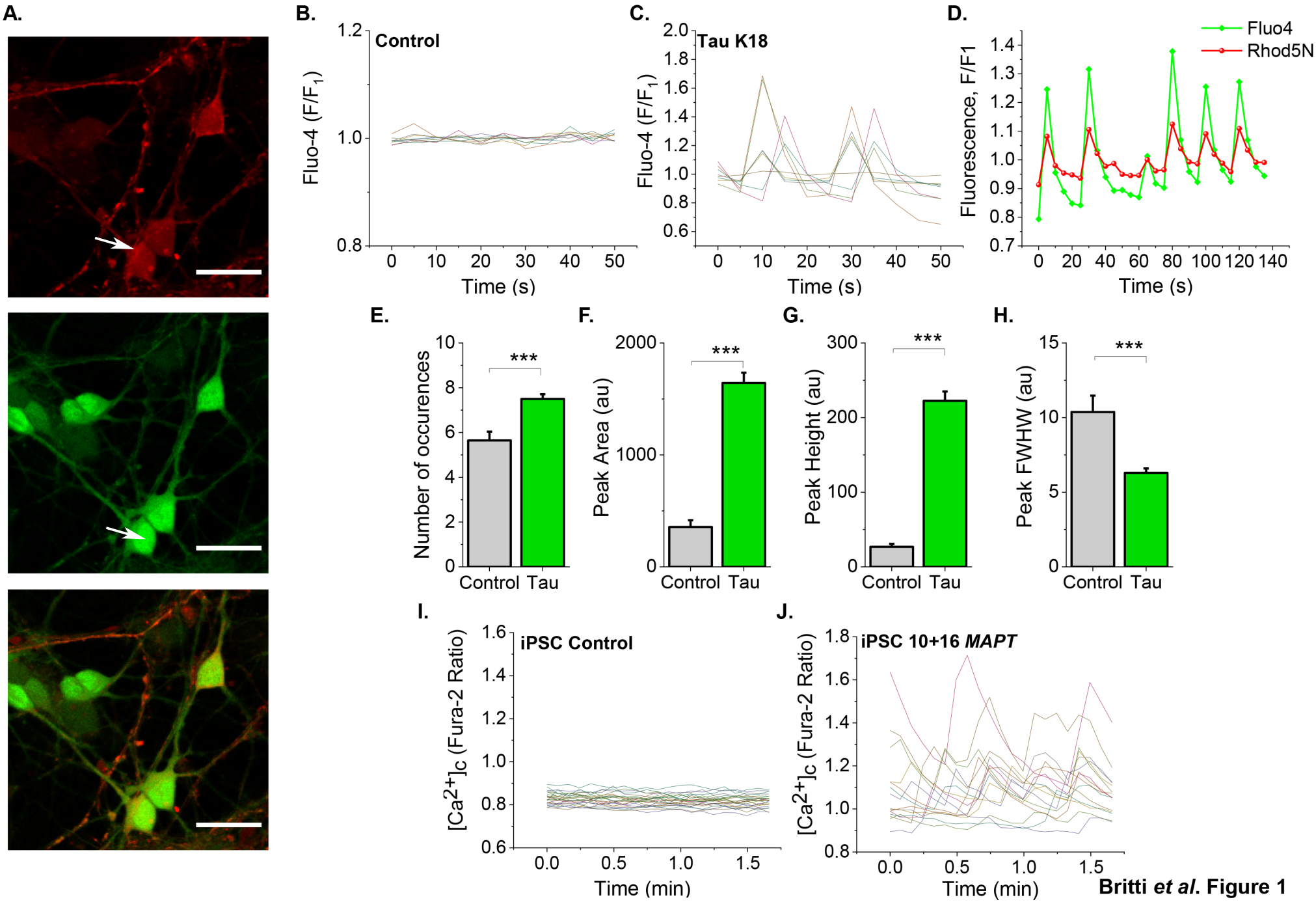

Britti *et al.* Figure 1

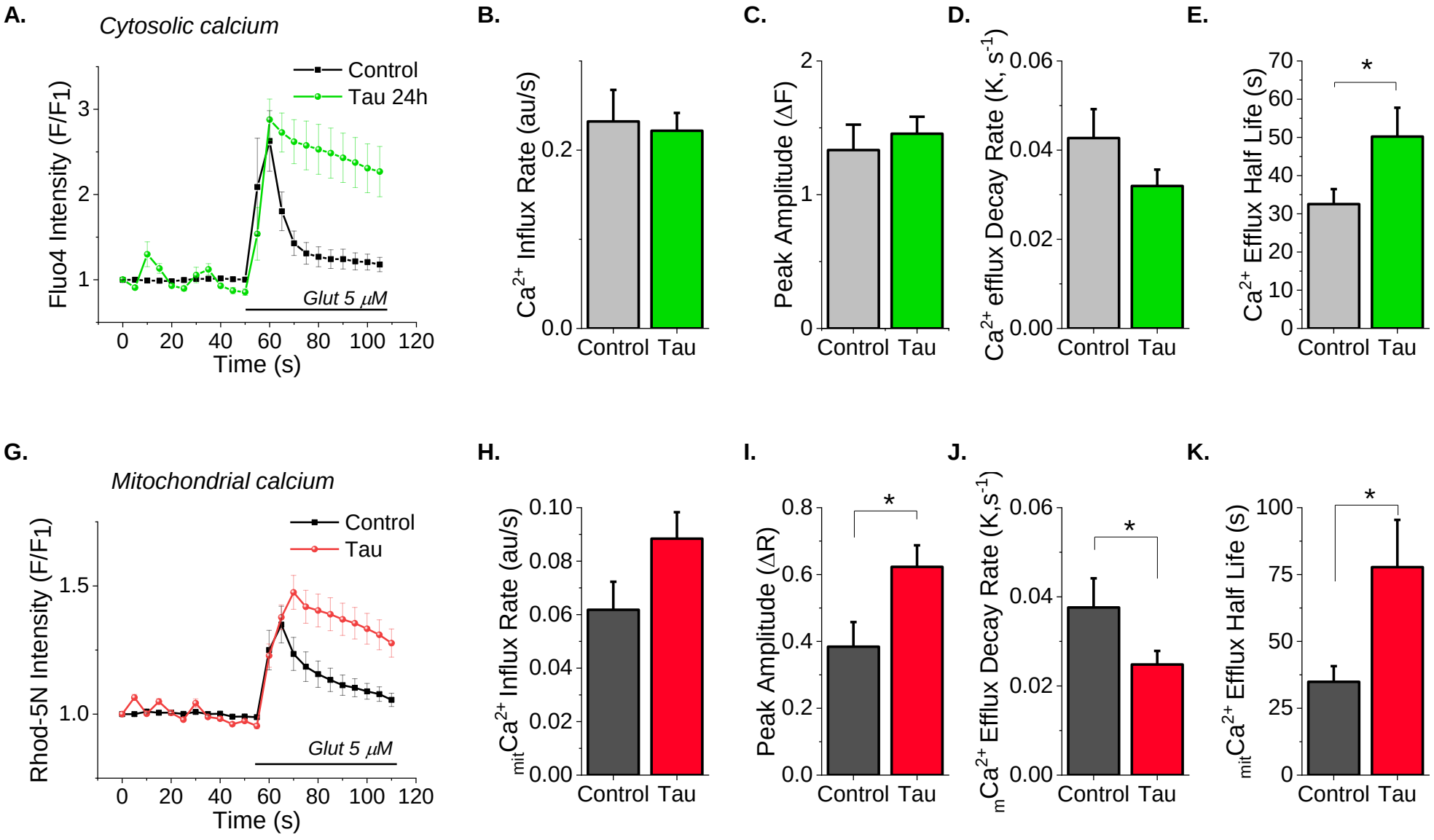

Britti *et al*. Figure 2

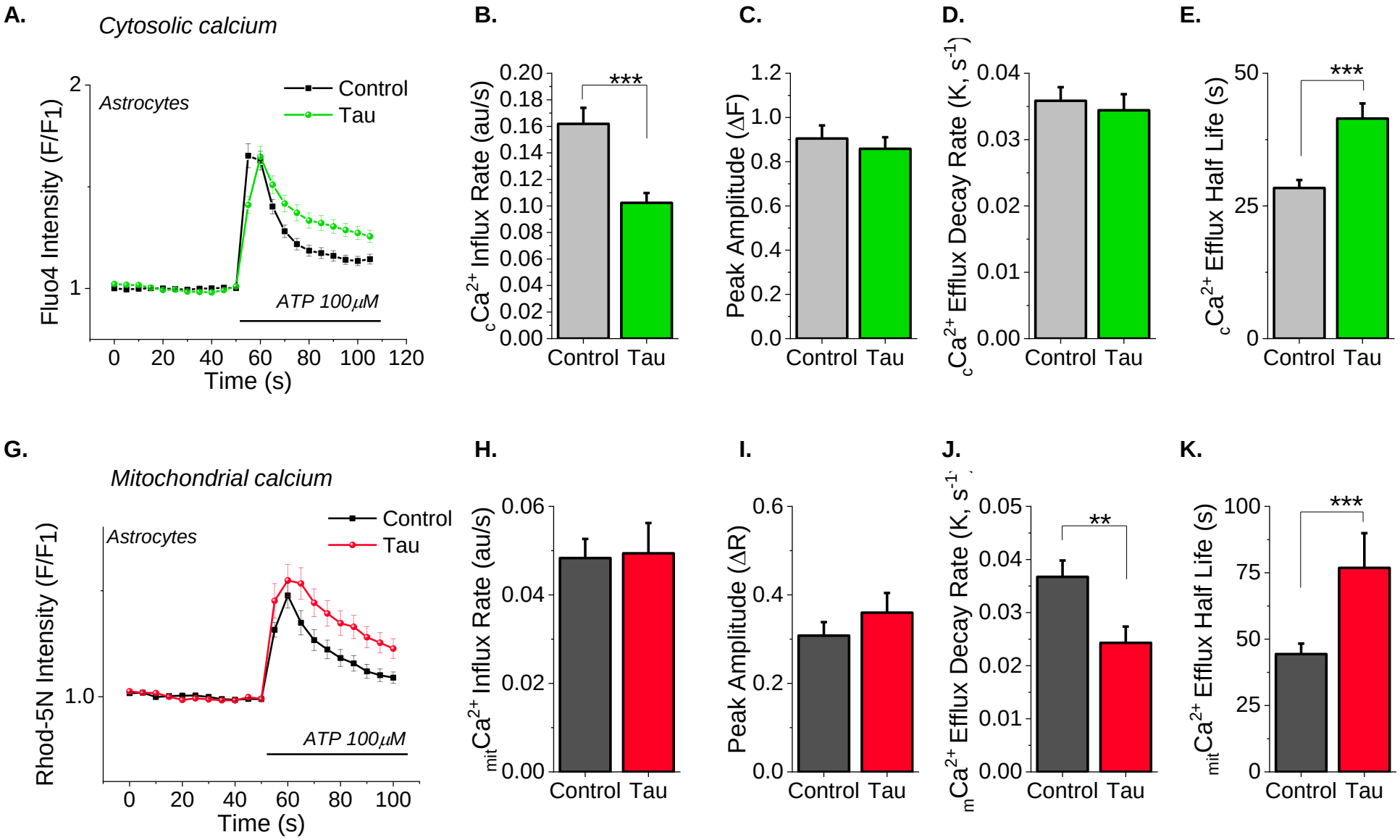

Britti *et al*. Figure 3

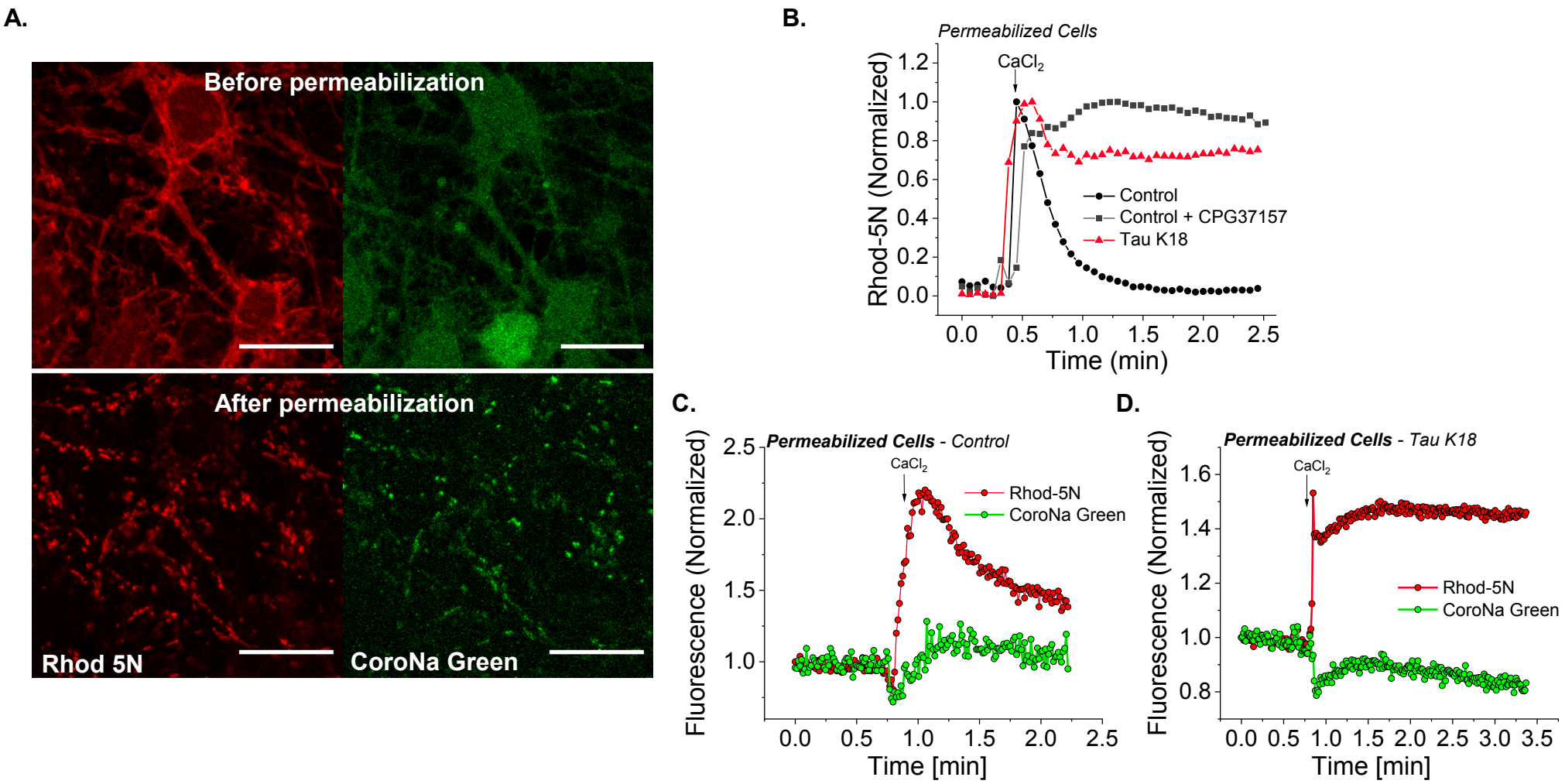

Britti *et al*. Figure 4

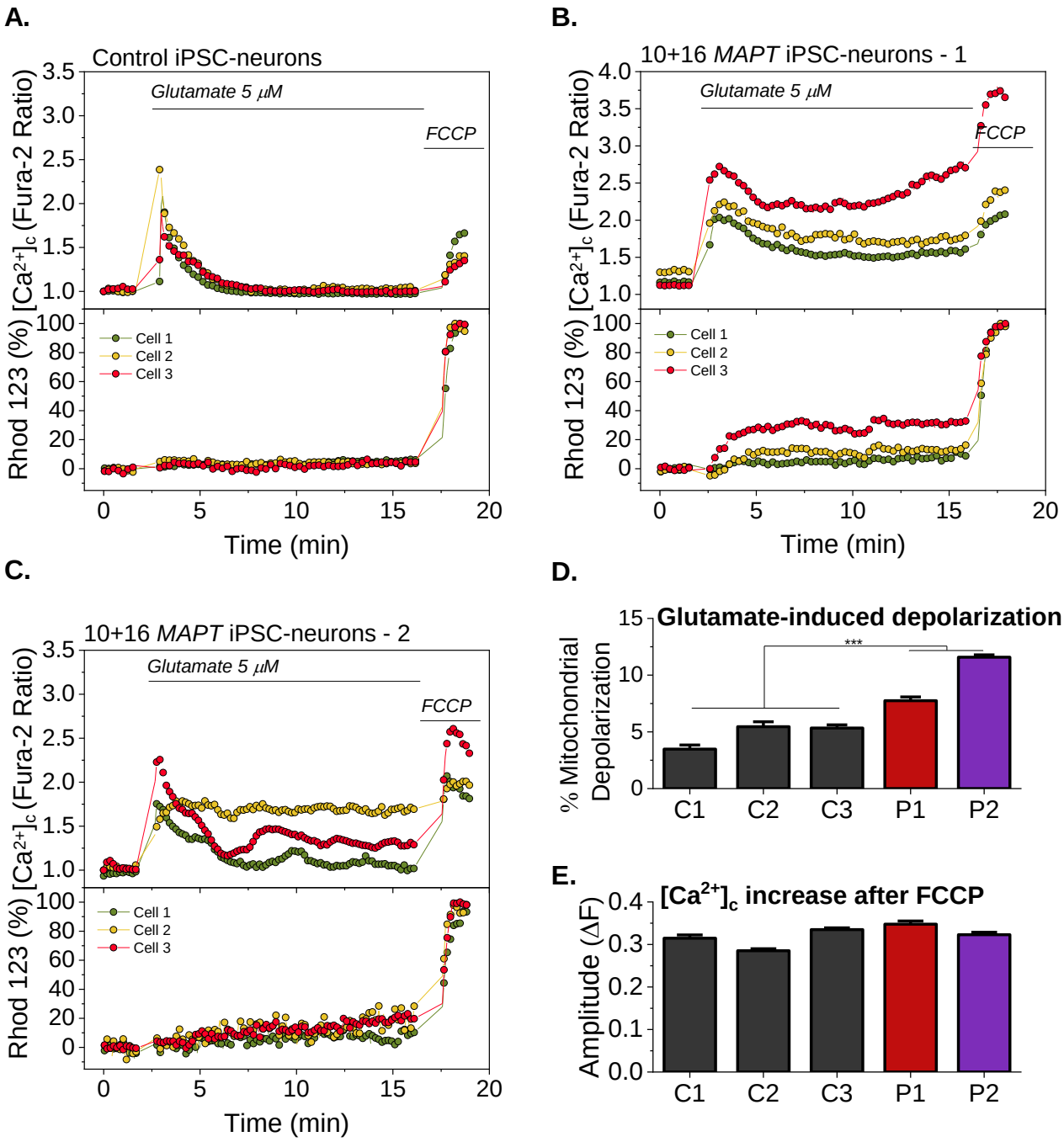

Britti *et al* Figure 5

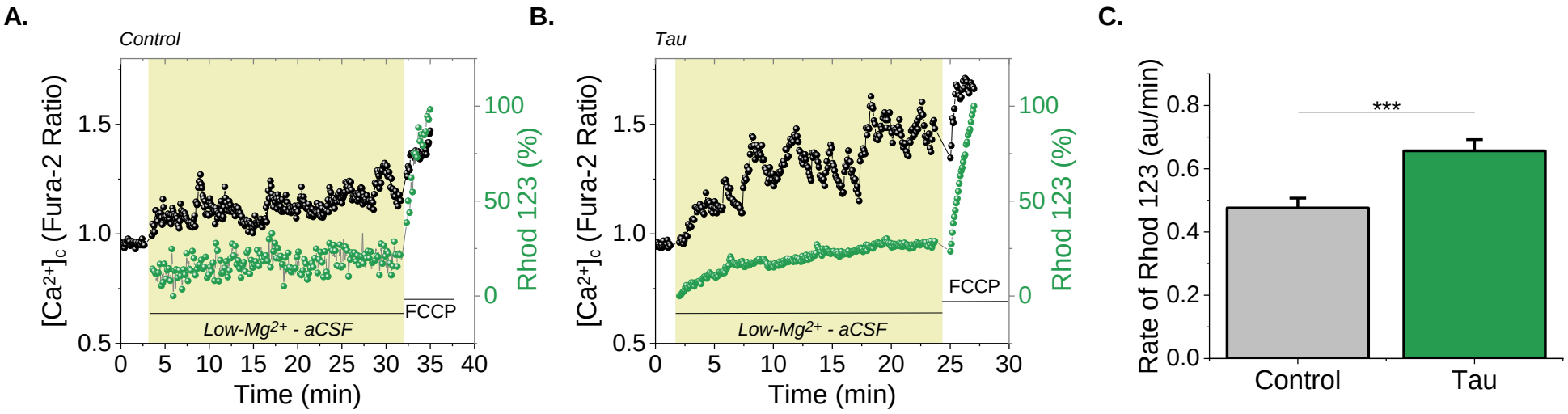

Britti *et al*. Figure 6

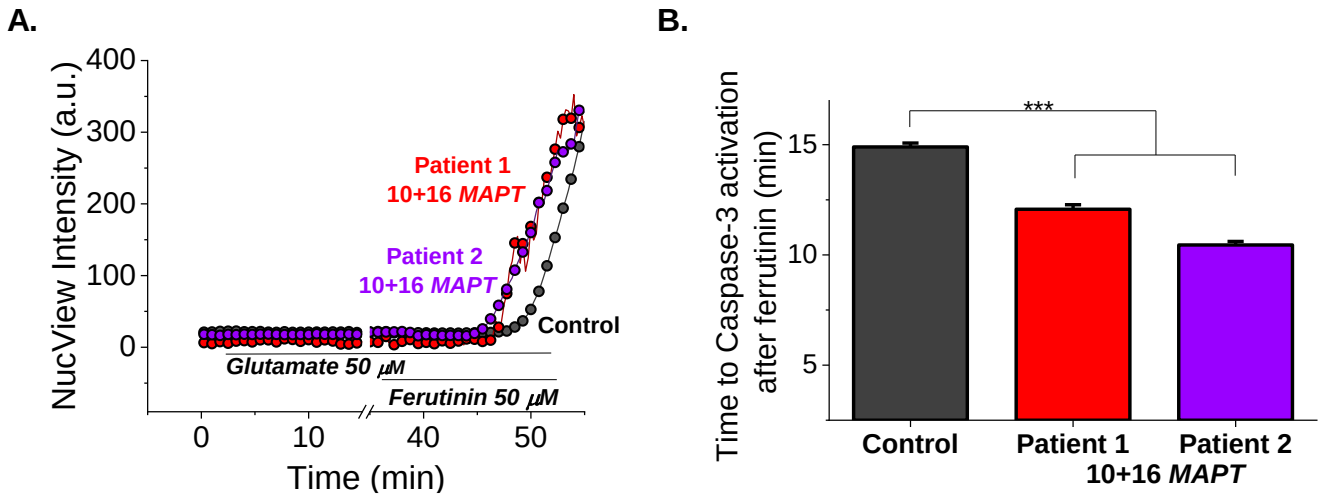

Britti *et al*. Figure 7